JPL PUBLICATION 85-29, VOLUME II

Proceedings of the Workshop on Identification and Control of Flexible Space Structures

Volume II

G. Rodriguez
Editor

April 1, 1985

National Aeronautics and
Space Administration

Jet Propulsion Laboratory
California Institute of Technology
Pasadena, California

PARAMETRIC STIFFNESS CONTROL OF FLEXIBLE STRUCTURES*

F. C. Moon+ and **R. H. Rand**++
Cornell University
Ithaca, NY 14853

ABSTRACT

We examine an unconventional method for control of flexible space structures using feedback control of certain elements of the stiffness matrix. The advantage of using this method of configuration control is that it can be accomplished in practical structures by changing the initial stress state in the structure. The initial stress state can be controlled hydraulically or by cables. The method leads, however, to nonlinear control equations. In particular, we examine a long slender truss structure under cable induced initial compression. Both analytical and numerical analyses are presented. Nonlinear analysis using center manifold theory and normal form theory is used to determine criteria on the nonlinear control gains for stable or unstable operation. The analysis is made possible by the use of the exact computer algebra system MACSYMA.

INTRODUCTION

The use of linear feedback forces to control linear flexible structures has been studied for over a decade, [1]-[4]. The efficacy of these methods has been demonstrated experimentally in the laboratory for a few cases (see e.g. Ref. 2, 3). However, the problem of applying linear feedback forces to an actual structure in space is formidable. For structures with significant bending deformations, forces transverse to the major axis of the structure are required such as small distributed rocket motors. An alternative is to use a scheme used in nature to control animal structural configuration, namely active control of their internal stress or muscles. In a man-made structure this analogy can be exploited by applying a self-equilibrated internal stress state through the use of cables or hydraulic actuators (Figure 1). The tension in cables can be controlled by DC servomotors and gear reducers. Such a method for control of internal stresses is suited to low frequency applications where control of the lowest modes of the structure is desired. From elementary structural theory it is known that the initial stress state can change the elastic stiffness matrix. The simplest example is the beam-column. In this case, the initial axial stress can even make the stiffness go to zero at buckling. Stiffness control of a

---

* Supported by a grant from the Air Force Office of Scientific Research, Mathematical Sciences and Aerospace Divisions.

+ Professor and Chairman, Theoretical and Applied Mechanics, Cornell University, Ithaca, NY 14853, U.S.A.

++Professor, Theoretical and Applied Mechanics, Cornell University, Ithaca, NY 14853, U.S.A.

vibrating string has been studied by Chen (5), and a two mode analysis of stiffness control has been presented by Fason et al. (6).

We propose the use of feedback to control elements of the stiffness matrix by controlling the internal stress. In one problem, we assume the structure is initially in a desired configuration and is impulsively disturbed. We examine the ability of several control laws to return the structure to its initial configuration. Both linear and nonlinear control laws are examined. Conditions for stable and unstable behavior of the system are derived.

STIFFNESS CONTROL - A SIMPLE EXAMPLE

The simplest structure for which an initial stress T can change the stiffness is the beam-column whose equation for the transverse displacement u is given below (Figure 2):

$$\frac{\partial^2}{\partial x^2} D \frac{\partial^2 u}{\partial x^2} + \gamma \frac{\partial^2 u}{\partial t^2} + \frac{\partial}{\partial x} T \frac{\partial u}{\partial x} = f + \frac{\partial g}{\partial x} \tag{1}$$

where f represents either distributed disturbances or linear control forces and g represents distributed torques such as those due to thermal or solar induced stresses. D is the bending stiffness and T is the axial compression induced by placing cables in tension along the beam. The mass density is γ .

Conventional control theory of flexible structures uses $f(x,t)$ to control the shape. In this paper we propose to use the initial stress or cable tension T to control the lowest mode. This eliminates the need for transverse control forces such as rockets or jets. When D and T are uniform along the beam, we have (neglecting distributed torques):

$$D \frac{\partial^4 u}{\partial x^4} + \gamma \frac{\partial^2 u}{\partial t^2} + T \frac{\partial^2 u}{\partial x^2} = f(x) \tag{2}$$

A single mode model may be derived using Galerkin's method where we assume the shape function is known

$$u(x,t) = A(t)U(x) \tag{3}$$

The equation for $A(t)$ takes the form,

$$\ddot{A} + (\omega^2 - \beta T)A = F(t) \tag{4}$$

Thus we can see that the stiffness term is linear in the initial stress T .

We propose a general control law for T , which includes both linear and nonlinear terms.

In general, the control law for the cable tension will have a lag due to servomotor or hydraulic system inertia or control circuit delay or stress waves propagating along the tension cables. (In a large structure the latter might not be negligible.) The tension will have a static and a dynamic part:

$$T = T_o + T_1(t) \tag{5}$$

where

$$\frac{1}{\alpha}\frac{dT_1}{dt} + T_1 = G(A,\dot{A}) \tag{6}$$

Three different control laws are examined

$$G = \Gamma_1 A + \Gamma_2 \dot{A} \tag{7}$$

$$G = \Gamma_3 A^2 + \Gamma_4 A\dot{A} + \Gamma_5 \dot{A}^2 \tag{8}$$

$$G = \frac{\Gamma_6 A\dot{A}}{(1 + \Gamma_7 A^2)} \tag{9}$$

Equations (4)-(6) constitute a nonlinear system of equations where the stiffness is controlled by a feedback parameter T, hence the term parametric stiffness control. This system is analogous to the Mathieu equation in which, however, the stiffness term is a known periodic function of time.

STIFFNESS CONTROL - GENERAL THEORY

For more general structures with a stiffness matrix $[k]$, mass matrix $[m]$ and a set of cable tensions $\{T\}$ one has a set of linear coupled equations for the generalized displacements or modal amplitudes $\{x\}$.

$$[m]\{\ddot{x}\} + [k]\{x\} = \{f(t)\} \tag{10}$$

where $\{f\}$ represents disturbances. In classic control theory of flexible structures one would use $\{f\}$ to provide control. In the present theory however we recognize that the elements of $[k]$ are linear functions of the tensions, i.e.,

$$k_{ij} = k^o_{ij} + \beta_{ijk}T_k \tag{11}$$

Thus one can try to vary the T_k to effect a change in any or all of the $\{x(t)\}$. To supplement these equations one requires a control law for the cable tensions. To account for lags in the cable control system, these control laws might take the form

$$\frac{1}{\alpha_k}\dot{T}_k + T_k = G_k(x_i, \dot{x}_j; S(t)) \tag{12}$$

where the $S(t)$ might be desired displacements. The system of equations (10)-(12) is clearly nonlinear. One can raise questions of observability, controllability, stability, etc. To effect all the modes one might require a combination of control force $\{f\}$ and stiffness control $\{T\}$. In the section below we examine a single mode problem and examine the question of stability for stiffness control alone.

ONE-MODE MODEL - STABILITY ANALYSIS

A) Nonlinear Quadratic Feedback Control

In this section we examine the stability of the equilibrium point at the origin under the quadratic feedback law (8). If one nondimensionalizes the modal amplitude so that the physical amplitude A is replaced by a dimensionless amplitude x, the equations (4), (6), and (8) can be put into the form of the rate of change of the state space vector $\underset{\sim}{r} = (x,y,z)^T$ where

$$\dot{x} = y \tag{13}$$

$$\dot{y} = -(1 + z)x \tag{14}$$

$$\dot{z} = -\alpha z + \alpha\left(G_{20}x^2 + G_{11}xy + G_{02}y^2\right) \tag{15}$$

where a general quadratic nonlinear control law has been assumed with control gains (G_{20}, G_{11}, G_{02}). We shall investigate the stability of this system of equations in the neighborhood of the equilibrium point at the origin $\underset{\sim}{r}=(0,0,0)$.

We note that the linearized system has eigenvalues i, $-i$, and $-\alpha$. The last eigenvalue corresponds to the decay of the servomotor transient $z \to 0$. This suggests that any motion starting close to the origin will eventually move down onto the x,y plane. To obtain a more precise description one must account for the nonlinear terms. This situation is clarified by the Center Manifold Theorem [7], which states that there exists a surface

$$z = f(x,y) \tag{16}$$

which is tangent to the x,y plane at the origin to which all solutions starting sufficiently close to the origin tend asymptotically. The surface is moreover invariant under the motion or flow given by (13)-(15).

In order to formally approximate (16) we expand $f(x,y)$ in a power series:

$$z = \sum_{i=2}^{\infty} \sum_{j=2}^{\infty} m_{ij}x^i y^j \tag{17}$$

The constant and linear terms in (17) are dropped in order that the surface be tangent to the x,y plane at the origin. The coefficients m_{ij} may be found by differentiating (17) with respect to t and using (13)-(15) and (17) to eliminate $\dot{x}$, $\dot{y}$, $\dot{z}$ and z. Collecting terms of like powers of $x^i y^j$ one can obtain the constants m_{ij}. Needless to say this procedure involves much algebra which is easily handled by the computer using the exact symbolic computer algebra system MACSYMA (see e.g. Rand [8]). Proceeding in this fashion we find that z consists of only even order terms. We expand (17) to powers up to fourth order and obtain expressions for the coefficients m_{20}, m_{11}, m_{02}, m_{04}, m_{31}, m_{22}, m_{13}, m_{04}. To illustrate the complexity of these coefficients we display four of them;

$$m_{20} = \frac{(\alpha^2 + 2)G_{20} + \alpha G_{11} + 2G_{02}}{\alpha^2 + 4}$$

$$m_{11} = \frac{-2\alpha G_{20} + \alpha^2 G_{11} + 2\alpha G_{02}}{\alpha^2 + 4}$$

$$m_{02} = \frac{2G_{20} - \alpha G_{11} + (\alpha^2 + 2)G_{02}}{\alpha^2 + 4} \tag{18}$$

$$m_{04} = -(2\alpha^6 G_{02}^2 - 10\alpha^5 G_{02}G_{11} + \alpha^4(32G_{02}G_{20} + 14G_{11}^2 + 16G_{02}^2) + \alpha^3(-92G_{11}G_{20} - 36G_{02}G_{11})$$
$$+\alpha^2(128G_{20}^2 + 96G_{02}G_{20} + 8G_{11}^2 + 64G_{02}^2) + \alpha(-176G_{11}G_{20} - 176G_{02}G_{11}) + 320G_{20}^2$$
$$+256G_{02}G_{20} - 64G_{02}^2)/(\alpha^8 + 28\alpha^6 + 240\alpha^4 + 832\alpha^2 + 1024)$$

The full set will be given in a forthcoming paper with more details.

The Center Manifold Theorem [7] states that the stability of the origin in the full three dimensional flow (13)-(15) is the same as the stability of the equilibrium point $x = y = 0$ in the flow on the center manifold. Thus, we are led to study the stability of the system of equations

$$\dot{x} = y$$
$$\dot{y} = -(1 + \sum_{i=0}^{4} \sum_{j=0}^{4} m_{ij} x^i y^j)x + O(7) \qquad i+j \le 4 \tag{19}$$

which may be considered as an oscillator with linear, cubic, and quintic forces. In the linearized case the eigenvalues $\pm i$ correspond to the "critical case" of Liapunov (see e.g., Minorsky, p. 150 [9]) and the stability cannot be determined on the basis of linear terms alone.

To study the stability of (19) we use the method of normal forms (see e.g., Guckenheimer and Holmes [10]). We posit a "near identity" transformation from x,y to u,v coordinates of the form

$$x = u + g(u,v)$$
$$y = v + h(u,v) \tag{20}$$

where g,h are polynomials with terms cubic and quintic in u,v having undetermined coefficients. Takens [11], has shown that it is always possible to transform systems like (19) (which have linear parts equivalent to simple harmonic oscillators) into a form which may be expressed simply in polar coordinates in the u,v plane:

$$\dot{r} = a_1 r^3 + a_2 r^5 + O(7) \tag{21}$$

$$\dot{\theta} = -1 + b_1 r^2 + b_2 r^4 + O(6) \tag{22}$$

where $u = r\cos\theta$, $v = r\sin\theta$. Although this procedure is straightforward, the choice of functions g,h involves solving sixteen algebraic equations. Again this task was made tractable by using MACSYMA.

The result of this computation is that the quantities a_1, a_2, b_1, b_2 in (21)-(22) are obtained in terms of the m_{ij}. We find

$$\begin{aligned} a_1 &= -m_{11}/8 \\ a_2 &= -(2m_{31} - m_{11}m_{20} + 2m_{13} - m_{02}m_{11})/32 \\ b_1 &= -(96m_{20} + 32m_{02})/256 \\ b_2 &= -(80m_{40} + 16m_{22} - 21m_{20}^2 + 18m_{02}m_{20} \\ &\quad - 5m_{11}^2 + 16m_{04} + 3m_{02}^2)/256 \end{aligned} \tag{23}$$

In terms of the original control gains in (15) we find

$$a_1 = \frac{2\alpha G_{20} - \alpha^2 G_{11} - 2\alpha G_{02}}{8\alpha^2 + 32} \tag{24}$$

$$\begin{aligned} a_2 = &-((2\alpha^5+48\alpha^3+96\alpha)G_{20}^2+((-\alpha^6-28\alpha^4-32\alpha^2)G_{11}+(4\alpha^5+64\alpha)G_{02})G_{20} \\ &+(2\alpha^5-8\alpha^3)G_{11}^2+(-\alpha^6-4\alpha^4-64\alpha^2)G_{02}G_{11}+(2\alpha^5+16\alpha^3-32\alpha)G_{02}^2) \\ &/(32\alpha^6+384\alpha^4+1536\alpha^2+2048) \end{aligned}$$

The equation for $\dot{r}$, (21), governs the stability of the origin and the existence of limit cycles, while the equation for $\dot{\theta}$, (22), specifies the frequency of the periodic motion corresponding to a limit cycle.

In particular the origin will be asymptotically stable if $a_1 < 0$ and unstable of $a_1 > 0$. If $a_1 = 0$ then the sign of a_2 determines the stability of the origin. Limit cycles correspond to equilibria of (21) and have a radius R given by

$$R^2 = -a_1/a_2 \qquad (25)$$

Since the power series expansions (17) and (19) are only valid in a neighborhood of the origin, the expression (25) can only be expected to be valid in a neighborhood of $a_1 = 0$. In terms of the control gains we have

$$R^2 = 4(\alpha^2+4)^2(2G_{20}-\alpha G_{11}-2G_{02})/(2\alpha^4G_{20}^2+48\alpha^2G_{20}^2+96G_{20}^2-\alpha^5G_{11}G_{20}$$
$$-28\alpha^3G_{11}G_{20}-32\alpha G_{11}G_{20}+4\alpha^4G_{02}G_{20}+64G_{02}G_{20}+2\alpha^4G_{11}^2-8\alpha^2G_{11}^2-\alpha^5G_{02}G_{11}$$
$$-4\alpha^3G_{02}G_{11}-64\alpha G_{02}G_{11}+2\alpha^4G_{02}^2+16\alpha^2G_{02}^2-32G_{02}^2) \qquad (26)$$

From (24) the condition for the stability of the equilibrium point at the origin is given by

$$-\frac{\alpha^2G_{11} + 2\alpha(G_{02}-G_{20})}{\alpha^2 + 4} < 0 \qquad (27)$$

In the limit of zero servomotor lag $\alpha \to \infty$, (27) requires that $G_{11} > 0$. This corresponds to a quadratic damping feedback law where in (7) $G = \Gamma_5 \dot{A}^2$. The stability condition (27) is a plane in control space (G_{11}, G_{02}, G_{20}) with a normal given by

$$\underset{\sim}{N} = (\alpha, 2, -2)$$

The maximum damping is obtained by choosing G_{11}, G_{02}, G_{20} so as to maximize the distance from this plane subject to the inequality (27).

Numerical integration of three specific quadratic feedback laws is shown in Figures 3, 4, and 5. A fourth order Runge-Kutta algorithm was used. In the stable case, we have $G_{02} = 1$, $G_{20} = 0$, $G_{11} = -1$, and $\alpha = 1$ which satisfies the stability criterion (27). We note the slow oscillatory decay which is characteristic of nonlinear quadratic damping (Figure 3).

In the second case (Figure 4) $\alpha = 3$, and the control system admits a limit cycle oscillation. In this case eq. (26) predicts a limit cycle radius of $R \simeq 0.86$ which agrees favorably with the numerical result. In the third example (Figure 5) we choose $G_{02} = G_{20} = 0$, $G_{11} = 1$. This case shows a stable damped spiral as in Figure 3.

B) Linear Feedback Control

The curious reader may wonder why we did not treat the case of the linear feedback (7) first. A linear feedback law, however, introduces quadratic terms in the dynamic equation (4) (or (13), (14)) in the limit of small lag $\alpha \to \infty$.

This introduces a saddle point in the phase plane and the system may not be globally bounded. However, using an analysis similar to that in the previous section we can show that the origin can be made stable in the limit of $\alpha \to \infty$. In this limit a linear feedback law

$$z = k_1 x + k_2 y \tag{28}$$

leads to the dynamic equation

$$\ddot{x} + x + k_1 x^2 + k_2 xy = 0 \tag{29}$$

Using normal form theory, an expression for the phase plane motion in polar coordinates can be found similar to (21)

$$\dot{r} = \frac{k_1 k_2 r^3}{8} + 0(5) \tag{30}$$

$$\dot{\theta} = \frac{1}{24}(k_2^2 + 10k_1^2)r^2 - 1 + 0(4) \tag{31}$$

By choosing $k_1 k_2 < 0$ a damped spiral motion can be obtained in the vicinity of the origin.

Numerical integration of the equation (29) confirms the result implied in (30), namely a stable spiral will result for $k_1 k_2 < 0$. This is illustrated in Figure 6. One can also observe in the Figure that for large initial conditions, the motion is not bounded because of the aforementioned saddle point at $y = 0$, $x = -1/k_1$.

C) Nonlinear Feedback -Rational Functions

As a final example we examine the case of stiffness control with a rational fraction feedback law where the equations take the form

$$\begin{aligned} \dot{x} &= y \\ \dot{y} &= -(1 + z)x \\ \dot{z} &= -\alpha z + \alpha P(x,y)/Q(x,y) \end{aligned} \tag{32}$$

where P, Q are polynomials in the amplitude and velocity variables x,y. As a special case, we choose a form of P,Q such that for large amplitude $x \to \infty$ and small feedback lag $\alpha \to \infty$, the system (32) looks like a damped linear oscillator. One choice is the following

$$\begin{aligned} \dot{x} &= y \\ \dot{y} &= -(1+z)x \\ \dot{z} &= -\alpha z + \alpha \Gamma xy/(1 + \eta x^2) \end{aligned} \tag{33}$$

When $|x| \to \infty$ and $\alpha \to \infty$ this looks like

$$\ddot{x} + \frac{\Gamma}{\eta}\dot{x} + x = 0 \tag{34}$$

For small $|x|$, (33) reduces to the previous example A with $G_{02} = G_{20} = 0$, $\Gamma = G_{11}$. From the previous analysis we require $\Gamma > 0$ for stability. By choosing optimum values for Γ, η one can hope to get the state vector to approach the origin with little oscillation.

A numerical simulation of the equations (33) was carried out using a fourth order Runge-Kutta algorithm for the case $\Gamma = 10$, $\eta = 1$. The results are shown in Figure 7. This control law has clear advantages over the quadratic case.

CONCLUSION

This pilot study on the possibility of stiffness control of structural dynamics illustrates some of the complexities of this concept. First the nature of stiffness control leads to a nonlinear dynamical problem even when the feedback law is linear. Second the study shows that nonlinear feedback laws may be more desirable than linear control when stiffness control is used. Finally we note the power of exact computer algebra (MACSYMA) in allowing one to use powerful nonlinear perturbation techniques such as normal form theory to analyze the stability of these nonlinear systems.

REFERENCES

1. Knyazev, A.S. and Tartakowskii, "Application of Electromechanical Feedback for the Damping of Flexural Vibration in Rods." Soviet Physics Acoustics Vol. II, pp. 150-154, October-December 1965.

2. Moon, F.C. and Dowell, E.H., "Control of Flutter Instability in a Continuous Elastic System Using Feedback." Proc. AIAA/ASME 11th Structures, Structural Dynamics, an Materials Conference, 1970.

3. Horikawa, H., Dowell, E.H., and Moon, F.C., "Active Feedback Control of a Beam Subjected to a Nonconservative Force." Int. J. Solids and Structures 14, pp. 821-839, 1978.

4. Meirovich, L. and Baruh, H., "Control of Self-Adjoint Distributed-Parameter System." J. Guidance, Control and Dynamics, Vol. 5, No. 1, 1982.

5. Chen, J. C., "Response of Large Space Structures with Stiffness Control," AAS/AIAA Paper No. 83-344, Astrodynamics Specialist Conference, Lake Placid, New York, August 1983.

6. Fanson, J.L., Chen, J.C. and Caughey, T.K., "Stiffness Control of Large Space Structures," This Conference.

7. Carr, J., "Applications of Centre Manifold Theory." Springer Verlag, 1981.

8. Rand, R.H., "Computer Algebra in Applied Mathematics: An Introduction to MACSYMA." Pitman Publishing, 1984.

9. Minorsky, N., "Nonlinear Oscillations." D. Van Nostrand Co., 1962.

10. Guckenheimer, J. and Holmes, P.J., "Nonlinear Oscillations, Dynamical Systems, and Bifurcations of Vector Fields." Springer-Verlag, 1983.

11. Takens, F., "Singularities of Vector Fields." Publ. Math. Inst. Hautes Etudes Sci. 43, 47-100, 1974.

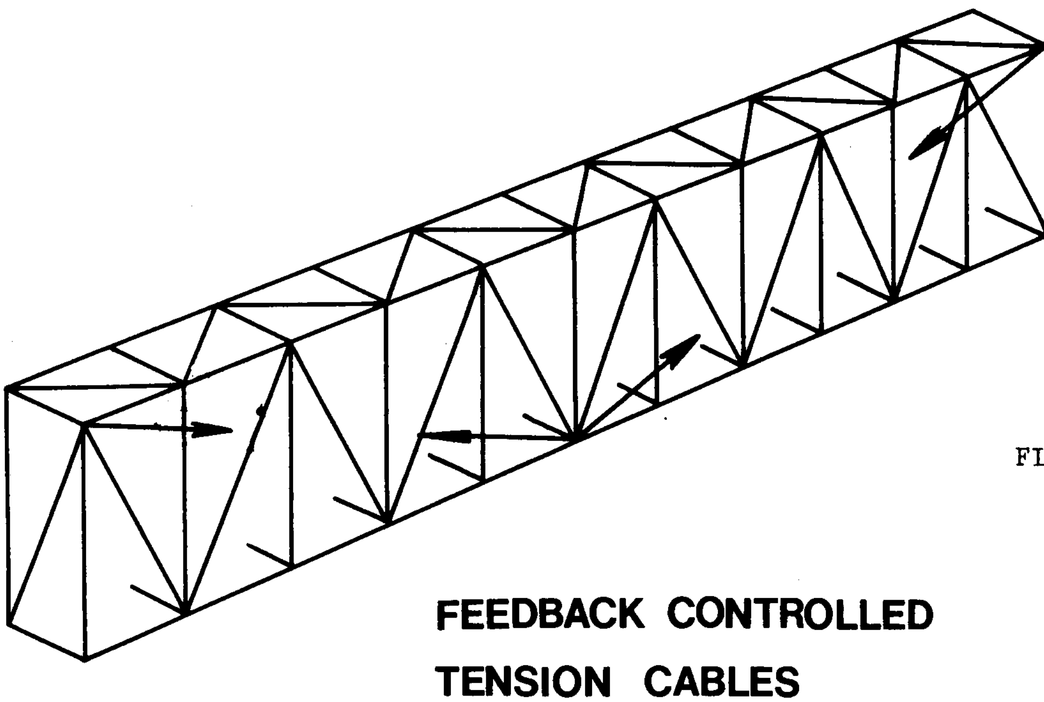

FIGURE 1

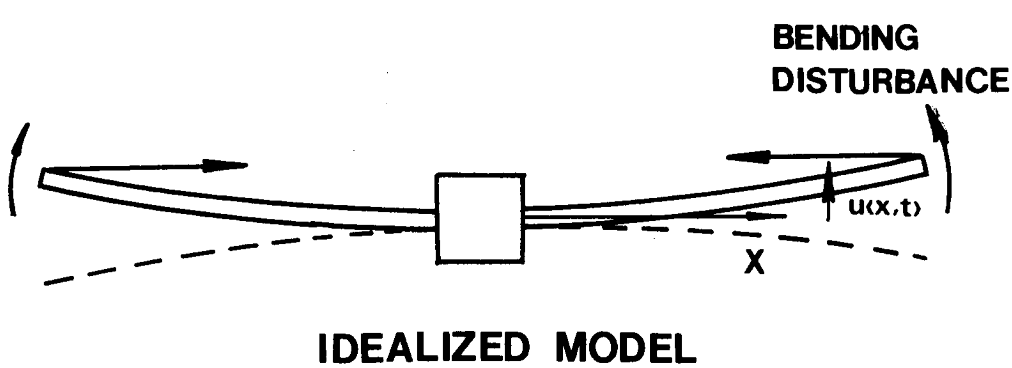

FIGURE 2

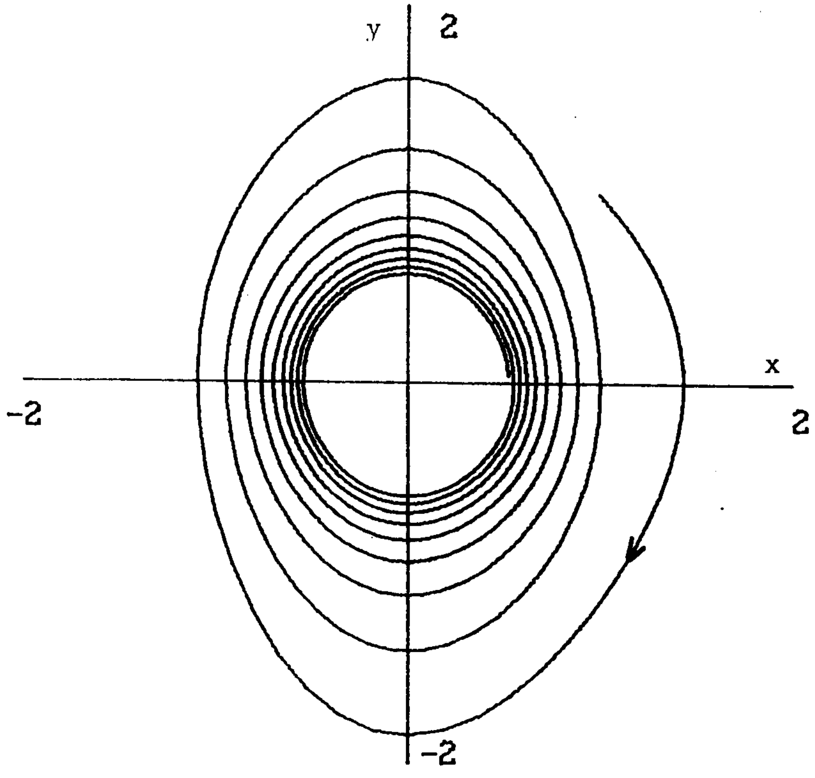

FIGURE 3. Numerical integration of eqs.(13)-(15) for parameter values $\alpha=1$, G02=1, G11=-1, G20=0. Note absence of limit cycle.

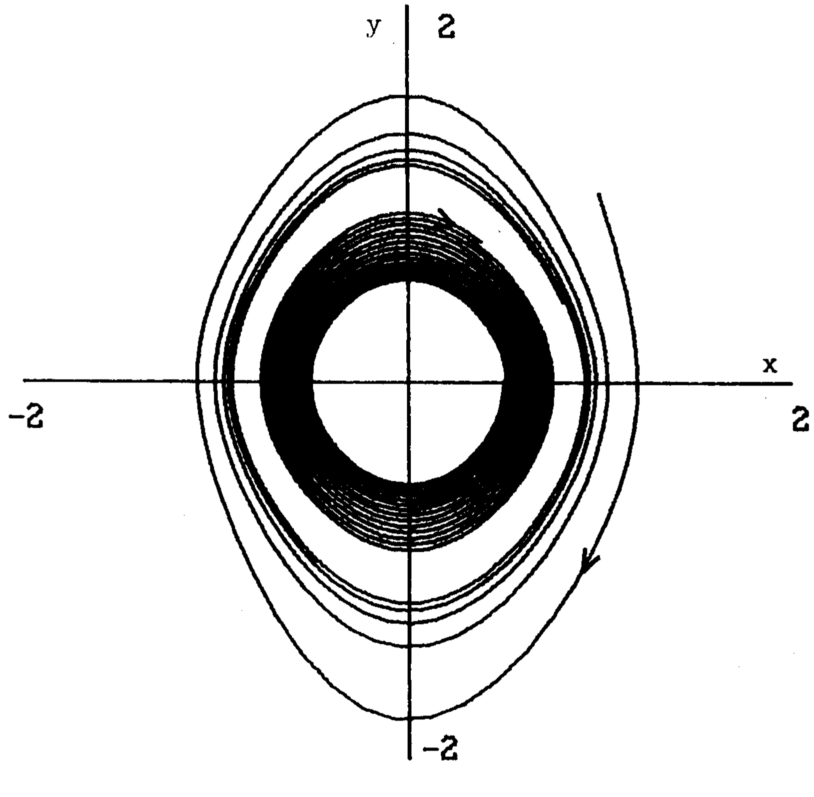

FIGURE 4. Numerical integration of eqs.(13)-(15) for parameter values $\alpha=3$, G02=1, G11=-1, G20=0. Presence of limit cycle indicated by growing inner trajectory and decaying outer trajectory.

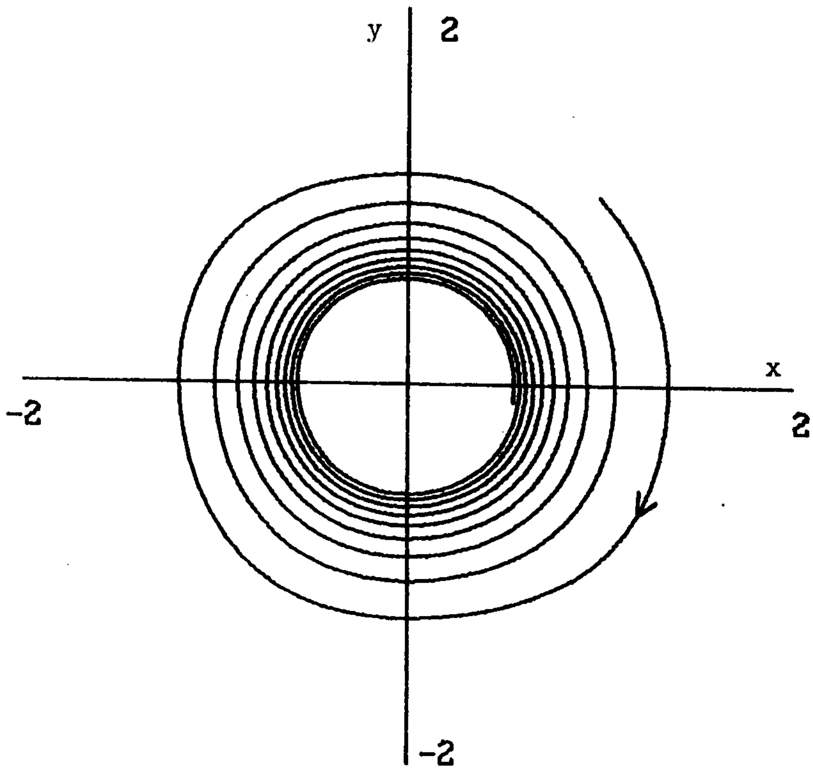

FIGURE 5. Numerical integration of eqs.(13)-(15) for parameter values $\alpha=1$, G02=0, G11=1, G20=0. The origin is aymptotically stable, in agreement with eq.(27).

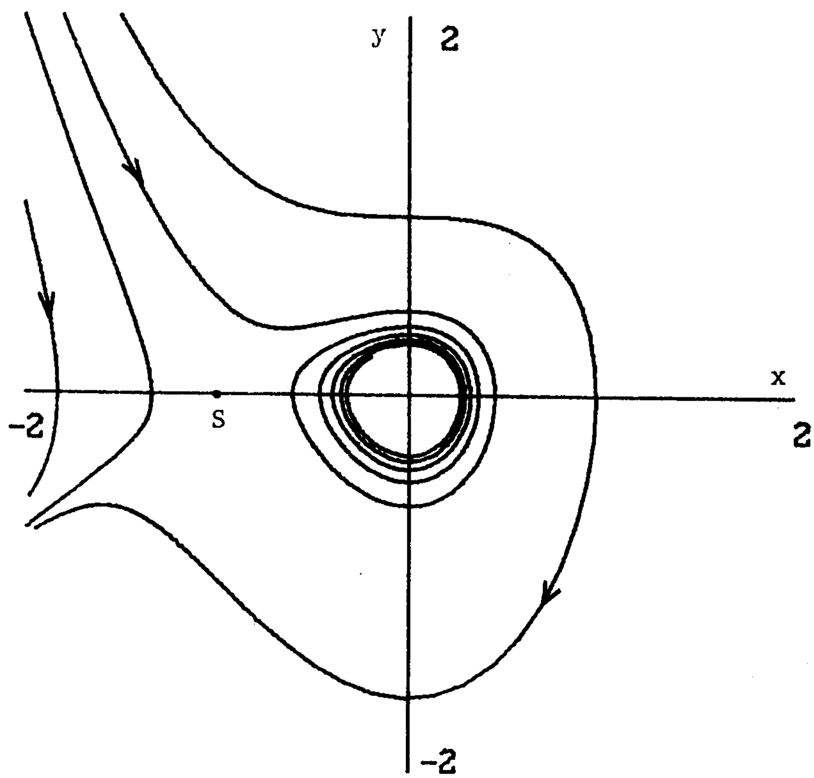

FIGURE 6. Numerical integration of eq.(29) with y=dx/dt for parameter values k1=1, k2=-1. Although the origin is aymptotically stable for sufficiently small initial conditions, the presence of a saddle S at x=-1, y=0 prevents the origin from exhibiting global asymptotic stability.

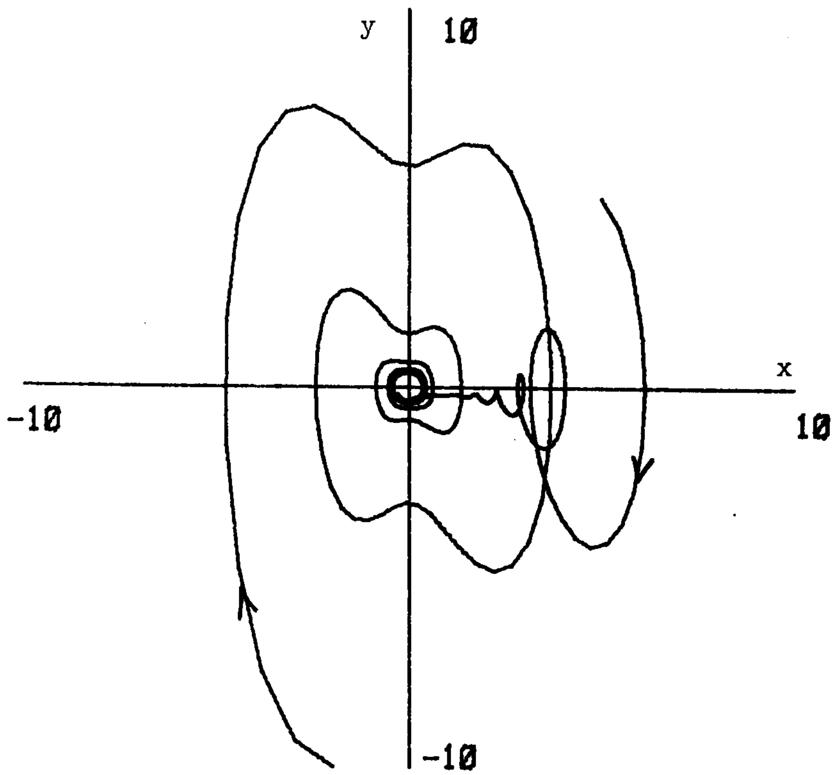

FIGURE 7. Numerical integration of eqs.(33) for parameter values $\alpha=1$, $\Gamma=10$, $\eta=1$.